Observation of an Energy-Dependent Difference in Elliptic Flow between Particles and Antiparticles in Relativistic Heavy Ion Collisions

L. Adamczyk *et al.* (STAR Collaboration)

Phys. Rev. Lett. **110**, 142301 — Published 2 April 2013

DOI: 10.1103/PhysRevLett.110.142301

Observation of an energy-dependent difference in elliptic flow between particles and anti-particles in relativistic heavy ion collisions

L. Adamczyk[1], J. K. Adkins[23], G. Agakishiev[21], M. M. Aggarwal[34], Z. Ahammed[53], I. Alekseev[19], J. Alford[22], C. D. Anson[31], A. Aparin[21], D. Arkhipkin[4], E. Aschenauer[4], G. S. Averichev[21], J. Balewski[26], A. Banerjee[53], Z. Barnovska [14], D. R. Beavis[4], R. Bellwied[49], M. J. Betancourt[26], R. R. Betts[10], A. Bhasin[20], A. K. Bhati[34], Bhattarai[48], H. Bichsel[55], J. Bielcik[13], J. Bielcikova[14], L. C. Bland[4], I. G. Bordyuzhin[19], W. Borowski[45], J. Bouchet[22], A. V. Brandin[29], S. G. Brovko[6], E. Bruna[57], S. Bültmann[32], I. Bunzarov[21], T. P. Burton[4], J. Butterworth[40], X. Z. Cai[44], H. Caines[57], M. Calderón de la Barca Sánchez[6], D. Cebra[6], R. Cendejas[35], M. C. Cervantes[47], P. Chaloupka[13], Z. Chang[47], S. Chattopadhyay[53], H. F. Chen[42], J. H. Chen[44], J. Y. Chen[9], L. Chen[9], J. Cheng[50], M. Cherney[12], A. Chikanian[57], W. Christie[4], P. Chung[14], J. Chwastowski[11], M. J. M. Codrington[48], R. Corliss[26], J. G. Cramer[55], H. J. Crawford[5], X. Cui[42], S. Das[16], A. Davila Leyva[48], L. C. De Silva[49], R. R. Debbe[4], T. G. Dedovich[21], J. Deng[43], R. Derradi de Souza[8], S. Dhamija[18], B. di Ruzza[4], L. Didenko[4], F. Ding[6], A. Dion[4], P. Djawotho[47], X. Dong[25], J. L. Drachenberg[52], J. E. Draper[6], C. M. Du[24], L. E. Dunkelberger[7], J. C. Dunlop[4], L. G. Efimov[21], M. Elnimr[56], J. Engelage[5], G. Eppley[40], L. Eun[25], O. Evdokimov[10], R. Fatemi[23], S. Fazio[4], J. Fedorisin[21], R. G. Fersch[23], P. Filip[21], E. Finch[57], Y. Fisyak[4], E. Flores[6], C. A. Gagliardi[47], D. R. Gangadharan[31], D. Garand[37], F. Geurts[40], A. Gibson[52], S. Gliske[2], O. G. Grebenyuk[25], D. Grosnick[52], A. Gupta[20], S. Gupta[20], W. Guryn[4], B. Haag[6], O. Hajkova[13], A. Hamed[47], L-X. Han[44], J. W. Harris[57], J. P. Hays-Wehle[26], S. Heppelmann[35], A. Hirsch[37], G. W. Hoffmann[48], D. J. Hofman[10], S. Horvat[57], B. Huang[4], H. Z. Huang[7], P. Huck[9], T. J. Humanic[31], G. Igo[7], W. W. Jacobs[18], C. Jena[30], E. G. Judd[5], S. Kabana[45], K. Kang[50], J. Kapitan[14], K. Kauder[10], H. W. Ke[9], D. Keane[22], A. Kechechyan[21], A. Kesich[6], D. P. Kikola[37], J. Kiryluk[25], I. Kisel[25], A. Kisiel[54], S. R. Klein[25], D. D. Koetke[52], T. Kollegger[15], J. Konzer[37], I. Koralt[32], W. Korsch[23], L. Kotchenda[29], P. Kravtsov[29], K. Krueger[2], I. Kulakov[25], L. Kumar[22], M. A. C. Lamont[4], J. M. Landgraf[4], K. D. Landry[7], S. LaPointe[56], J. Lauret[4], A. Lebedev[4], R. Lednicky[21], J. H. Lee[4], W. Leight[26], M. J. LeVine[4], C. Li[42], W. Li[44], X. Li[37], X. Li[46], Y. Li[50], Z. M. Li[9], L. M. Lima[41], M. A. Lisa[31], F. Liu[9], T. Ljubicic[4], W. J. Llope[40], R. S. Longacre[4], Y. Lu[42], X. Luo[9], A. Luszczak[11], G. L. Ma[44], Y. G. Ma[44], D. M. M. D. Madagodagettige Don[12], D. P. Mahapatra[16], R. Majka[57], S. Margetis[22], C. Markert[48], H. Masui[25], H. S. Matis[25], D. McDonald[40], T. S. McShane[12], S. Mioduszewski[47], M. K. Mitrovski[4], Y. Mohammed[47], B. Mohanty[30], M. M. Mondal[47], M. G. Munhoz[41], M. K. Mustafa[37], M. Naglis[25], B. K. Nandi[17], Md. Nasim[53], T. K. Nayak[53], J. M. Nelson[3], L. V. Nogach[36], J. Novak[28], G. Odyniec[25], A. Ogawa[4], K. Oh[38], A. Ohlson[57], V. Okorokov[29], E. W. Oldag[48], R. A. N. Oliveira[41], D. Olson[25], M. Pachr[13], B. S. Page[18], S. K. Pal[53], Y. X. Pan[7], Y. Pandit[10], Y. Panebratsev[21], T. Pawlak[54], B. Pawlik[33], H. Pei[10], C. Perkins[5], W. Peryt[54], P. Pile[4], M. Planinic[58], J. Pluta[54], N. Poljak[58], J. Porter[25], A. M. Poskanzer[25], C. B. Powell[25], C. Pruneau[56], N. K. Pruthi[34], M. Przybycien[1], P. R. Pujahari[17], J. Putschke[56], H. Qiu[25], S. Ramachandran[23], R. Raniwala[39], S. Raniwala[39], R. L. Ray[48], C. K. Riley[57], H. G. Ritter[25], J. B. Roberts[40], O. V. Rogachevskiy[21], J. L. Romero[6], J. F. Ross[12], L. Ruan[4], J. Rusnak[14], N. R. Sahoo[53], P. K. Sahu[16], I. Sakrejda[25], S. Salur[25], A. Sandacz[54], J. Sandweiss[57], E. Sangaline[6], A. Sarkar[17], J. Schambach[48], R. P. Scharenberg[37], A. M. Schmah[25], B. Schmidke[4], N. Schmitz[27], T. R. Schuster[15], J. Seger[12], P. Seyboth[27], N. Shah[7], E. Shahaliev[21], M. Shao[42], B. Sharma[34], M. Sharma[56], S. S. Shi[9], Q. Y. Shou[44], E. P. Sichtermann[25], R. N. Singaraju[53], M. J. Skoby[18], D. Smirnov[4], N. Smirnov[57], D. Solanki[39], P. Sorensen[4], U. G. deSouza[41], H. M. Spinka[2], B. Srivastava[37], T. D. S. Stanislaus[52], J. R. Stevens[26], R. Stock[15], M. Strikhanov[29], B. Stringfellow[37], A. A. P. Suaide[41], M. C. Suarez[10], M. Sumbera[14], X. M. Sun[25], Y. Sun[42], Z. Sun[24], B. Surrow[46], D. N. Svirida[19], T. J. M. Symons[25], A. Szanto de Toledo[41], J. Takahashi[8], A. H. Tang[4], Z. Tang[42], L. H. Tarini[56], T. Tarnowsky[28], J. H. Thomas[25], J. Tian[44], A. R. Timmins[49], D. Tlusty[14], M. Tokarev[21], S. Trentalange[7], R. E. Tribble[47], P. Tribedy[53], B. A. Trzeciak[54], O. D. Tsai[7], J. Turnau[33], T. Ullrich[4], D. G. Underwood[2], G. Van Buren[4], G. van Nieuwenhuizen[26], J. A. Vanfossen, Jr.[22], R. Varma[17], G. M. S. Vasconcelos[8], F. Videbæk[4], Y. P. Viyogi[53], S. Vokal[21], S. A. Voloshin[56], A. Vossen[18], M. Wada[48], F. Wang[37], G. Wang[7], H. Wang[4], J. S. Wang[24], Q. Wang[37], X. L. Wang[42], Y. Wang[50], G. Webb[23], J. C. Webb[4], G. D. Westfall[28], C. Whitten Jr.[7], H. Wieman[25], S. W. Wissink[18], R. Witt[51], Y. F. Wu[9], Z. Xiao[50], W. Xie[37], K. Xin[40], H. Xu[24], N. Xu[25], Q. H. Xu[43], W. Xu[7], Y. Xu[42], Z. Xu[4], L. Xue[44], Y. Yang[24], Y. Yang[9], P. Yepes[40], L. Yi[37], K. Yip[4], I-K. Yoo[38], M. Zawisza[54], H. Zbroszczyk[54], J. B. Zhang[9], S. Zhang[44], X. P. Zhang[50], Y. Zhang[42], Z. P. Zhang[42], F. Zhao[7], J. Zhao[44], C. Zhong[44], X. Zhu[50], Y. H. Zhu[44], Y. Zoulkarneeva[21], M. Zyzak[25]

(STAR Collaboration)

[1]*AGH University of Science and Technology, Cracow, Poland*

[2]*Argonne National Laboratory, Argonne, Illinois 60439, USA*

[3]University of Birmingham, Birmingham, United Kingdom
[4]Brookhaven National Laboratory, Upton, New York 11973, USA
[5]University of California, Berkeley, California 94720, USA
[6]University of California, Davis, California 95616, USA
[7]University of California, Los Angeles, California 90095, USA
[8]Universidade Estadual de Campinas, Sao Paulo, Brazil
[9]Central China Normal University (HZNU), Wuhan 430079, China
[10]University of Illinois at Chicago, Chicago, Illinois 60607, USA
[11]Cracow University of Technology, Cracow, Poland
[12]Creighton University, Omaha, Nebraska 68178, USA
[13]Czech Technical University in Prague, FNSPE, Prague, 115 19, Czech Republic
[14]Nuclear Physics Institute AS CR, 250 68 Řež/Prague, Czech Republic
[15]University of Frankfurt, Frankfurt, Germany
[16]Institute of Physics, Bhubaneswar 751005, India
[17]Indian Institute of Technology, Mumbai, India
[18]Indiana University, Bloomington, Indiana 47408, USA
[19]Alikhanov Institute for Theoretical and Experimental Physics, Moscow, Russia
[20]University of Jammu, Jammu 180001, India
[21]Joint Institute for Nuclear Research, Dubna, 141 980, Russia
[22]Kent State University, Kent, Ohio 44242, USA
[23]University of Kentucky, Lexington, Kentucky, 40506-0055, USA
[24]Institute of Modern Physics, Lanzhou, China
[25]Lawrence Berkeley National Laboratory, Berkeley, California 94720, USA
[26]Massachusetts Institute of Technology, Cambridge, MA 02139-4307, USA
[27]Max-Planck-Institut für Physik, Munich, Germany
[28]Michigan State University, East Lansing, Michigan 48824, USA
[29]Moscow Engineering Physics Institute, Moscow Russia
[30]National Institute of Science Education and Research, Bhubaneswar 751005, India
[31]Ohio State University, Columbus, Ohio 43210, USA
[32]Old Dominion University, Norfolk, VA, 23529, USA
[33]Institute of Nuclear Physics PAN, Cracow, Poland
[34]Panjab University, Chandigarh 160014, India
[35]Pennsylvania State University, University Park, Pennsylvania 16802, USA
[36]Institute of High Energy Physics, Protvino, Russia
[37]Purdue University, West Lafayette, Indiana 47907, USA
[38]Pusan National University, Pusan, Republic of Korea
[39]University of Rajasthan, Jaipur 302004, India
[40]Rice University, Houston, Texas 77251, USA
[41]Universidade de Sao Paulo, Sao Paulo, Brazil
[42]University of Science & Technology of China, Hefei 230026, China
[43]Shandong University, Jinan, Shandong 250100, China
[44]Shanghai Institute of Applied Physics, Shanghai 201800, China
[45]SUBATECH, Nantes, France
[46]Temple University, Philadelphia, Pennsylvania, 19122
[47]Texas A&M University, College Station, Texas 77843, USA
[48]University of Texas, Austin, Texas 78712, USA
[49]University of Houston, Houston, TX, 77204, USA
[50]Tsinghua University, Beijing 100084, China
[51]United States Naval Academy, Annapolis, MD 21402, USA
[52]Valparaiso University, Valparaiso, Indiana 46383, USA
[53]Variable Energy Cyclotron Centre, Kolkata 700064, India
[54]Warsaw University of Technology, Warsaw, Poland
[55]University of Washington, Seattle, Washington 98195, USA
[56]Wayne State University, Detroit, Michigan 48201, USA
[57]Yale University, New Haven, Connecticut 06520, USA and
[58]University of Zagreb, Zagreb, HR-10002, Croatia

Elliptic flow (v_2) values for identified particles at mid-rapidity in Au+Au collisions, measured by the STAR experiment in the Beam Energy Scan at RHIC at $\sqrt{s_{NN}} = 7.7$–62.4 GeV, are presented. A beam-energy dependent difference of the values of v_2 between particles and corresponding anti-particles was observed. The difference increases with decreasing beam energy and is larger for baryons compared to mesons. This implies that, at lower energies, particles and anti-particles are not consistent with the universal number-of-constituent-quark (NCQ) scaling of v_2 that was observed at $\sqrt{s_{NN}} = 200$ GeV.

PACS numbers: 25.75.Ld. 25.75. Nq

Lattice Quantum Chromodynamics (QCD) predicts that at sufficiently high temperatures, T, and/or high baryonic chemical potentials, μ_B, normal nuclear matter will undergo a phase transition to a state of matter where quarks and gluons are deconfined, called the Quark-Gluon Plasma (QGP) [1]. This transition is important for understanding the early evolution of the universe [2]. A Beam Energy Scan (BES) program [3] has been carried out at the Relativistic Heavy Ion Collider (RHIC) facility to study the QCD phase structure over a large range in T and μ_B.

Particle production in heavy ion collisions with respect to the event plane (EP) can be characterized by the following Fourier expansion:

$$\frac{dN}{d(\phi-\Psi)} \propto 1 + 2\sum_{n\geq 1} v_n^{obs}\cos\left[n(\phi-\Psi)\right], \qquad (1)$$

where ϕ is the azimuthal angle of the particles, n the harmonic number, v_n^{obs} the observed Fourier coefficient which has to be corrected for the EP resolution to get v_n, and Ψ the reconstructed EP azimuthal angle [4, 5]. The second harmonic coefficient is denoted as elliptic flow, v_2 [4].

Elliptic flow measurements have been used to conclude that strongly interacting partonic matter is produced in Au+Au collisions at $\sqrt{s_{NN}} = 200$ GeV and that v_2 develops in the early, partonic, stage. This conclusion is based in part on the observed scaling of v_2 versus the transverse momentum, p_T, with the number of constituent-quarks (NCQ) [6–9] for hadrons at intermediate p_T (2 to 5 GeV/c). Deviations from such a scaling for identified hadron $v_2(p_T)$ at lower beam energies is thus an indication for the absence of a deconfined phase [3].

In a hydrodynamic picture, v_2 arises in non-central heavy ion collisions due to an initial pressure gradient, which is directly connected to the eccentricity. This leads to particle emission predominantly in the direction of the maximum of the pressure gradient. During the expansion of the system the pressure gradient decreases, which means that elliptic flow primarily probes the early stage of a heavy ion collision.

For Au+Au collisions at $\sqrt{s_{NN}} = 200$ GeV, a mass ordering in $v_2(p_T)$ between the different particle species was observed at low transverse momenta ($p_T < 2$ GeV/c) [6, 10, 11]. This behaviour can be described by non-viscous hydrodynamic calculations [12–17]. The relative mass ordering can be suppressed by using the reduced transverse kinetic energy ($m_T - m_0$) instead of p_T, with $m_T = \sqrt{p_T^2 + m_0^2}$ and m_0 being the mass of the particle. At large ($m_T - m_0$), a splitting in $v_2(m_T - m_0)$ between baryons and mesons was observed which cannot be described by hydrodynamic calculations. This splitting can be explained, in part, by assuming that the particle production occurs via coalescence of constituent quarks [18].

The v_2 values for $\pi^{\pm}$, $K^{\pm}$, K_S^0, p, $\bar{p}$, ϕ, Λ, $\overline{\Lambda}$, Ξ^-, $\overline{\Xi}^+$, Ω^-, $\overline{\Omega}^+$ measured at mid-rapidity in minimum bias Au+Au collisions will be reported. The data were recorded by STAR, the Solenoidal Tracker at RHIC, for $\sqrt{s_{NN}} = 7.7$, 11.5, 19.6, 27, 39, and 62.4 GeV in the years 2010 and 2011 as part of the BES program [3].

STAR is a multi-purpose experiment at RHIC with a complete azimuthal coverage. The main detectors used for the data analysis were the Time-Projection Chamber (TPC) [19] for tracking and particle identification at pseudo-rapidities $|\eta| < 1.0$, and the Time-of-Flight (TOF) detector, which was especially important to identify charged particles at intermediate momenta. A minimum bias trigger was defined using a coincidence of hits in the Zero Degree Calorimeters, Vertex Position Detectors, or Beam-Beam Counters [20, 21]. To suppress events from collisions with the beam pipe (radius 3.95 cm), an upper limit cut on the radial position of the reconstructed primary vertex of 2 cm was applied. In addition, the z-position of the vertices was limited to values less than ± 70 cm. Collisions within a 0–80% centrality range of the total reaction cross section were selected for the analysis. The centrality definition is based on a comparison between the measured track multiplicity within $|\eta| < 0.5$ and a Glauber Monte-Carlo simulation [20].

The particle identification and yield extraction for long-lived charged hadrons (p, $\bar{p}$, $\pi^{\pm}$, $K^{\pm}$) was based on a combination of the ionization energy loss, dE/dx, in the TPC, the reconstructed momentum (p), and the squared mass, m^2, from the TOF detector [21]. Short-lived particles which decay within the detector acceptance such as ϕ, Λ, $\overline{\Lambda}$, Ξ^-, $\overline{\Xi}^+$, Ω^-, $\overline{\Omega}^+$, and K_s^0 were identified using the invariant mass technique. The combinatorial background to the weakly decaying particles like Λ and Ξ was reduced by topological reconstruction. The remaining combinatorial background was fit and subtracted with the mixed event technique [21].

The event plane was reconstructed using the procedure described in Ref. [4]. In order to reduce the effects of non-flow contributions arising mainly from Hanbury-Brown Twiss correlations and Coulomb interactions, the event plane angles were estimated for two sub-events separated by an additional η-gap instead of using the full TPC event plane method [21]. For such an "η-sub-EP" reconstruction, one uses only the particles from the opposite η hemisphere with respect to the particle of interest and outside of an additional η-gap of $|\eta| > 0.05$. The non-flow contributions were studied for the six beam energies by comparing different methods of extracting v_2 for inclusive charged hadrons [20]. The four particle cumulant $v_2\{4\}$ strongly suppresses non-flow contributions. It has been shown that the difference between $v_2(\eta\text{-sub})$ and $v_2\{4\}$ is 10–20% for 19.2, 27, and 39 GeV and decreases with decreasing energy. All observed values (v_2^{obs}) were corrected on an event-by-event basis using the EP

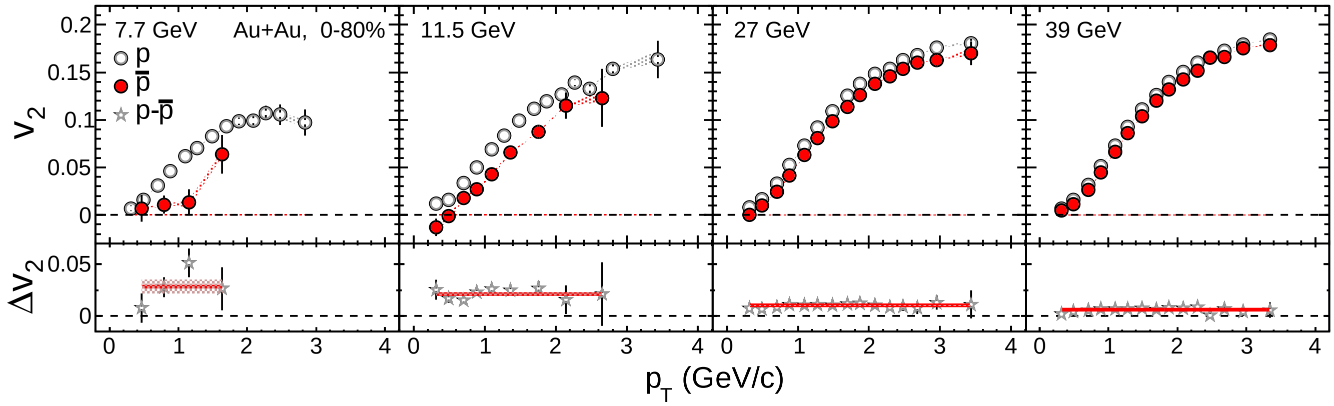

FIG. 1. (Color online) The elliptic flow v_2 of protons and anti-protons as a function of the transverse momentum, p_T, for 0–80% central Au+Au collisions. The lower panels show the difference in $v_2(p_T)$ between the particles and anti-particles. The solid curves are fits with a horizontal line. The shaded areas depict the magnitude of the systematic errors.

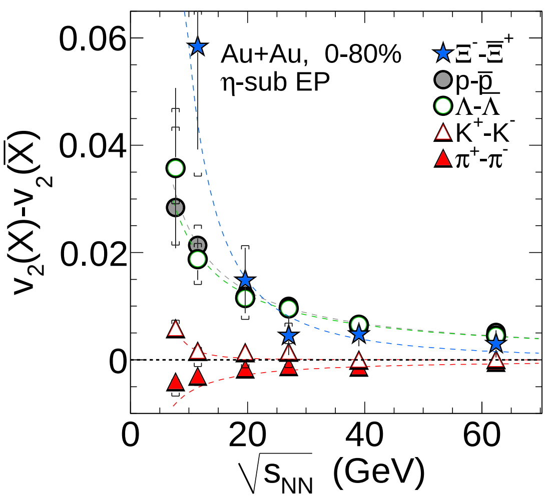

FIG. 2. (Color online) The difference in v_2 between particles (X) and their corresponding anti-particles ($\overline{\mathrm{X}}$) (see legend) as a function of $\sqrt{s_{NN}}$ for 0–80% central Au+Au collisions. The dashed lines in the plot are fits with a power-law function. The error bars depict the combined statistical and systematic errors.

resolution [22] which was calculated by comparing the two η-sub-EP angles [20].

For each particle species, the cuts used for particle identification and background suppression were varied to estimate the systematic uncertainties. The errors were also estimated by varying the methods used to flatten the EP, to obtain the yields, and to extract the v_2 values. A more detailed description of the detector setup and the analysis can be found in Ref. [21].

In Fig. 1, the p_T dependence of the proton and anti-proton v_2 is shown for Au+Au collisions at $\sqrt{s_{NN}} =$ 7.7, 11.5, 27, and 39 GeV. At all energies, the v_2 values increase with increasing p_T. At $p_T = 2$ GeV/c, the magnitude of v_2 for protons increases with energy from about 0.10 at 7.7 GeV to 0.15 at 39 GeV. Lower values of $v_2(p_T)$ are observed for anti-protons compared to protons at all energies. The difference in the v_2 values for protons and anti-protons increases with decreasing beam energy. The lower panels of Fig. 1 show the p_T dependence of the difference in v_2 for protons and anti-protons. No significant p_T dependence is observed, as characterized by the horizontal line fits. The negative values of the anti-proton v_2 at low p_T at $\sqrt{s_{NN}} = 11.5$ GeV could be influenced by absorption in the medium [23]. Suppressed or negative v_2 values are also observed at $\sqrt{s_{NN}} = 7.7$ GeV for different centralities [21].

The $v_2(p_T)$ behaviour for $\Lambda(uds)$, $\overline{\Lambda}(\bar{u}\bar{d}\bar{s})$ and $\Xi^-(dss)$, $\overline{\Xi}^+(\bar{d}\bar{s}\bar{s})$ is similar to that for protons (uud) and anti-protons ($\bar{u}\bar{u}\bar{d}$). In all cases, the baryon anti-particle v_2 is lower than the corresponding particle v_2. The $v_2(p_T)$ difference for Λ and $\overline{\Lambda}$ is in agreement with previous STAR results at $\sqrt{s_{NN}} = 62.4$ GeV [7]. For the mesons $\pi^+(u\bar{d})$, $\pi^-(\bar{u}d)$, and $K^+(u\bar{s})$, $K^-(\bar{u}s)$, the differences are smaller than those for the baryons (the anti-particle convention from [24] is used for mesons). At $\sqrt{s_{NN}} = 7.7$ GeV, the $v_2(p_T)$ difference between K^+ and K^- is a factor 5–6 smaller as compared to the baryons, with K^+ having a systematically larger $v_2(p_T)$ than the K^-. On the other hand, the $v_2(p_T)$ of the π^- is larger than the $v_2(p_T)$ of the π^+. However, the magnitude of the difference for pions as a function of energy is similar to that for the kaons. The details of the p_T dependence of the difference in v_2 between particles and corresponding anti-particles can be found in Ref. [21].

Figure 2 summarizes the variation of the p_T independent difference in v_2 between particles and corresponding anti-particles with $\sqrt{s_{NN}}$. Here, $v_2(X) - v_2(\overline{X})$ denotes the horizontal line fit values of the difference in $v_2(p_T)$ between particles X (p, Λ, Ξ^-, π^+, K^+) and corresponding anti-particles $\overline{X}$ ($\bar{p}$, $\overline{\Lambda}$, $\overline{\Xi}^+$, π^-, K^-). Larger v_2 values are found for particles than for antiparticles, except for pions for which the opposite ordering is observed. A monotonic increase of the magnitude of $\Delta v_2 = v_2(X) - v_2(\overline{X})$ with

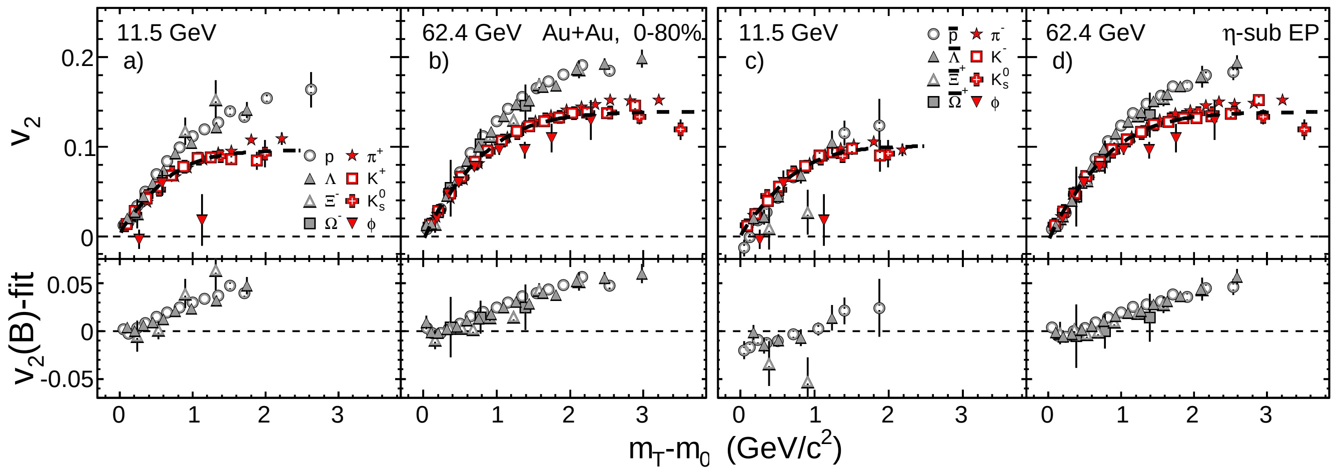

FIG. 3. (Color online) The upper panels depict the elliptic flow, v_2, as a function of reduced transverse mass, $(m_T - m_0)$, for particles, frames a) and b), and anti-particles, frames c) and d), in 0-80% central Au+Au collisions at $\sqrt{s_{NN}}$ = 11.5 and 62.4 GeV. Simultaneous fits to the mesons except the pions are shown as the dashed lines. The difference of the baryon v_2 and the meson fits are shown in the lower panels.

decreasing beam energy is observed. The data can be described by a power-law function.

While in Au+Au collisions at $\sqrt{s_{NN}}$ = 200 GeV a single NCQ scaling can be observed for particles and anti-particles, the observed difference in v_2 at lower beam energies demonstrates that this common NCQ scaling of particles and anti-particles splits. Such a breaking of the NCQ scaling could indicate increased contributions from hadronic interactions in the system evolution with decreasing beam energy. The energy dependence of $v_2(X) - v_2(\overline{X})$ could also be accounted for by considering an increase in nuclear stopping power with decreasing $\sqrt{s_{NN}}$ if the v_2 of transported quarks (quarks coming from the incident nucleons) is larger than the v_2 of produced quarks [25, 26]. Theoretical calculations [27] suggest that the difference between particles and anti-particles could be accounted for by mean field potentials where the K^- and $\bar{p}$ feel an attractive force while the K^+ and p feel a repulsive force.

Most of the published theoretical calculations can reproduce the basic pattern, but fail to quantitatively reproduce the measured v_2 difference [25–28]. So far, none of the theory calculations describes the observed ordering of the particles. Therefore, more accurate calculations from theory are needed to distinguish between the different possibilities. Other possible reasons for the observation that the π^- $v_2(p_T)$ is larger than the π^+ $v_2(p_T)$ is the Coulomb repulsion of π^+ by the mid-rapidity net-protons (only at low p_T) and the chiral magnetic effect in finite baryon-density matter [29]. Simulations have to be carried out to quantify if those effects can explain our observations.

In Ref. [21], the study of the centrality dependence of Δv_2 for protons and anti-protons is extended to investigate, if different production rates for protons and anti-protons as a function of centrality could cause the observed differences. It was observed that the differences, Δv_2, are significant at all centralities.

The $v_2(m_T - m_0)$ and possible NCQ scaling was also investigated for particles and anti-particles separately. Figure 3 shows v_2 as a function of the reduced transverse mass, $(m_T - m_0)$, for various particles and anti-particles at $\sqrt{s_{NN}}$ = 11.5 and 62.4 GeV. The baryons and mesons are clearly separated for $\sqrt{s_{NN}}$ = 62.4 GeV at $(m_T - m_0) > 1$ GeV/c^2. While the effect is present for particles at $\sqrt{s_{NN}}$ = 11.5 GeV, no such separation is observed for the anti-particles at this energy in the measured $(m_t - m_0)$ range up to 2 GeV/c^2. The lower panels of Fig. 3 depict the difference of the baryon v_2 relative to a fit to the meson v_2 data with the pions excluded from the fit. The anti-particles at $\sqrt{s_{NN}}$ = 11.5 GeV show a smaller difference compared to the particles. At $\sqrt{s_{NN}}$ = 11.5 GeV the difference becomes negative for the anti-particles at $(m_T - m_0) < 1$ GeV/c^2 but the overall trend is still similar to the one of the particles and to $\sqrt{s_{NN}}$ = 62.4 GeV.

In Fig. 4, the $v_2(m_T - m_0)$ values scaled on both axes with the number of constituent-quarks are presented for $\sqrt{s_{NN}}$ = 11.5 and 62.4 GeV. A simultaneous fit [30] to p, $\bar{p}$, Λ, and $\bar{\Lambda}$ at a given energy is shown as the dashed line. The differences between data and corresponding fits are shown in the lower panels. The general scaling holds, except for the ϕ mesons, for the various particles, as shown in panels a) and b) with deviations of $\sim$10% at a $(m_T - m_0)/n_q$ value of 0.7 GeV/c^2. A significant change in the scaling behaviour can be observed between baryon and anti-baryon v_2 from $\sqrt{s_{NN}}$ = 62.4 GeV to 11.5 GeV, as shown in panels c) and d). The ϕ mesons are also an exception to the trend of other hadrons. At the highest $(m_T - m_0)/n_q$ values, the ϕ meson data point for $\sqrt{s_{NN}}$ = 11.5 GeV (p_T = 1.9 GeV/c) is 2.3σ lower than those of the other hadrons. This is comparable to

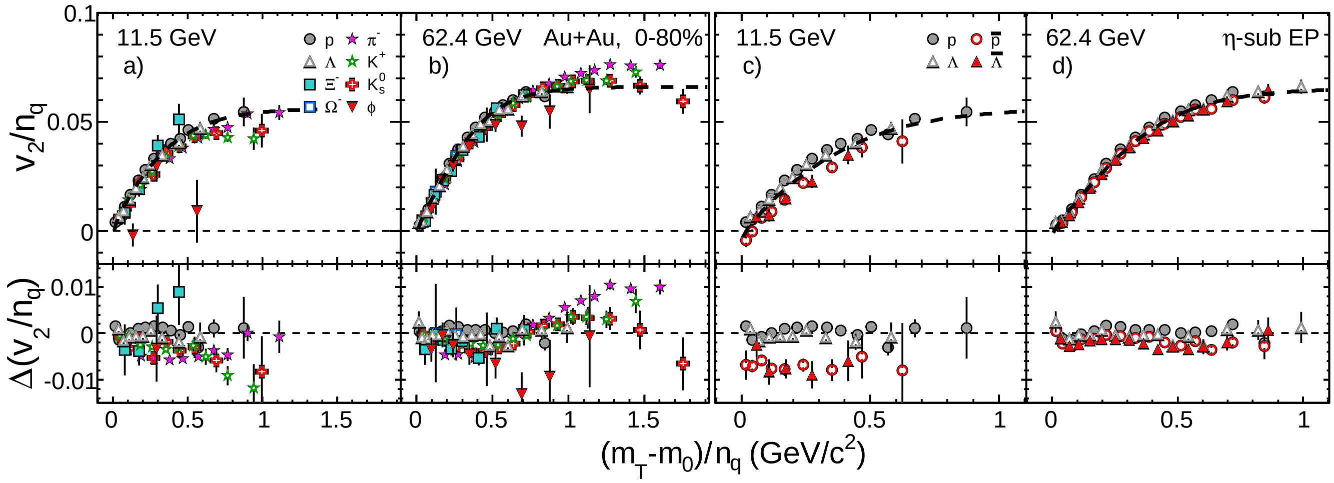

FIG. 4. (Color online) The number-of-constituent quark scaled elliptic flow $(v_2/n_q)((m_T - m_0)/n_q)$ for 0–80% central Au+Au collisions at $\sqrt{s_{NN}} = 11.5$ and 62.4 GeV for selected particles, frames a) and b), and a direct comparison between selected baryons and anti-baryons, frames c) and d). The dashed lines are simultaneous fits [30] to p, $\bar{p}$, Λ, and $\bar{\Lambda}$ at a given energy. The lower panels depict the differences to the fits. Some data points for ϕ are out of the plot range in the lower panels.

the observed deviation at $\sqrt{s_{NN}} = 7.7$ GeV ($p_T = 1.7$ GeV/c) by 1.8σ [21]. The smaller v_2 values of the $\phi(s\bar{s})$ meson, which has a smaller hadronic interaction cross section [31], may indicate that hadronic interactions become more important than partonic effects for the systems formed at collision energies $\lesssim 11.5$ GeV [32, 33].

In summary, the first observation of a beam-energy dependent difference in $v_2(p_T)$ between particles and corresponding anti-particles for minimum bias $\sqrt{s_{NN}} = 7.7$–62.4 GeV Au+Au collisions at mid-rapidity is reported. The difference increases with decreasing beam energy. Baryons show a larger difference compared to mesons. The relative values of v_2 for charged pions have the opposite trend to the values of charged kaons. It is concluded that, at the lower energies, particles and anti-particles are no longer consistent with the single NCQ scaling that was observed for $\sqrt{s_{NN}} = 200$ GeV. However, for the group of particles the NCQ scaling holds within ±10% while for the group of anti-particles the difference between baryon and meson v_2 continues to decrease to lower energies. We further observed that the ϕ meson v_2 at the highest measured $m_T - m_0$ value is low compared to other hadrons at $\sqrt{s_{NN}} = 7.7$ and 11.5 GeV with 1.8σ and 2.3σ, respectively.

We thank the RHIC Operations Group and RCF at BNL, the NERSC Center at LBNL and the Open Science Grid consortium for providing resources and support. This work was supported in part by the Offices of NP and HEP within the U.S. DOE Office of Science, the U.S. NSF, the Sloan Foundation, CNRS/IN2P3, FAPESP CNPq of Brazil, Ministry of Ed. and Sci. of the Russian Federation, NNSFC, CAS, MoST, and MoE of China, GA and MSMT of the Czech Republic, FOM and NWO of the Netherlands, DAE, DST, and CSIR of India, Polish Ministry of Sci. and Higher Ed., Korea Research Foundation, Ministry of Sci., Ed. and Sports of the Rep. of Croatia, and RosAtom of Russia, and VEGA of Slovakia.

[1] D. J. Gross, R. D. Pisarski, and L. G. Yaffe, Rev. Mod. Phys. **53**, 43 (1981).
[2] C. Aktas and I. Yilmaz, Gen. Rel. Grav. **43**, 1577 (2011).
[3] M. M. Aggarwal *et al.* [STAR Collaboration], arXiv:1007.2613 [nucl-ex] (2010).
[4] A. M. Poskanzer and S. A. Voloshin, Phys. Rev. C **58**, 1671 (1998).
[5] S. Voloshin and Y. Zhang, Z. Phys. C **70**, 665 (1996).
[6] J. Adams *et al.* [STAR Collaboration], Phys. Rev. Lett. **95**, 122301 (2005).
[7] B. I. Abelev *et al.* [STAR Collaboration], Phys. Rev. C **75**, 054906 (2007).
[8] S. A. Voloshin, A. M. Poskanzer, and R. Snellings, arXiv:0809.2949 [nucl-ex] (2008).
[9] A. Adare *et al.* [PHENIX Collaboration], Phys. Rev. C **85**, 064914 (2012).
[10] C. Adler *et al.* [STAR Collaboration], Phys. Rev. Lett. **87**, 182301 (2001).
[11] J. Adams *et al.* [STAR Collaboration], Phys. Rev. Lett. **92**, 052302 (2004).
[12] P. Huovinen, P. F. Kolb, U. W. Heinz, P. V. Ruuskanen, and S. A. Voloshin, Phys. Lett. B **503**, 58 (2001).
[13] C. Nonaka, R. J. Fries, and S. A. Bass, Phys. Lett. B **583**, 73 (2004).
[14] T. Hirano and Y. Nara, Phys. Rev. C **69**, 034908 (2004).
[15] C. Shen and U. Heinz, Phys. Rev. C **85**, 054902 (2012) [Erratum ibid. C **86**, 049903 (2012)].
[16] B. Schenke, S. Jeon, and C. Gale, Phys. Rev. Lett. **106**, 042301 (2011).
[17] M. Csanad, T. Csorgo and B. Lorstad, Nucl. Phys. A

742, 80 (2004).

[18] D. Molnar and S. A. Voloshin, Phys. Rev. Lett. **91**, 092301 (2003).

[19] K. H. Ackermann et al., Nucl. Instr. and Meth. A 499, 624 (2003).

[20] L. Adamczyk *et al.* [STAR Collaboration], Phys. Rev. C **86**, 054908 (2012).

[21] L. Adamczyk *et al.* [STAR Collaboration], arXiv:1301.2348.

[22] H. Masui and A. Schmah, arXiv:1212.3650 [nucl-ex] (2012).

[23] F. Wang, M. Nahrgang and M. Bleicher, Phys. Rev. C **85**, 031902 (2012).

[24] J. Beringer *et al.* [Particle Data Group Collaboration], Phys. Rev. D **86**, 010001 (2012).

[25] J. C. Dunlop, M. A. Lisa, and P. Sorensen, Phys. Rev. C **84**, 044914 (2011).

[26] J. Steinheimer, V. Koch and M. Bleicher, Phys. Rev. C **86**, 044903 (2012).

[27] J. Xu, L. -W. Chen, C. M. Ko, and Z. -W. Lin, Phys. Rev. C **85**, 041901 (2012).

[28] T. Song, S. Plumari, V. Greco, C. M. Ko and F. Li, arXiv:1211.5511 [nucl-th].

[29] Y. Burnier, D. E. Kharzeev, J. Liao and H. -U. Yee, Phys. Rev. Lett. **107**, 052303 (2011).

[30] X. Dong, S. Esumi, P. Sorensen, N. Xu, and Z. Xu, Phys. Lett. B **597**, 328 (2004).

[31] A. Sibirtsev, H. -W. Hammer, U. -G. Meissner and A. W. Thomas, Eur. Phys. J. A **29**, 209 (2006).

[32] B. Mohanty and N. Xu, J. Phys. G **36**, 064022 (2009).

[33] M. Nasim, B. Mohanty and N. Xu, arXiv:1301.1375 [nucl-ex].